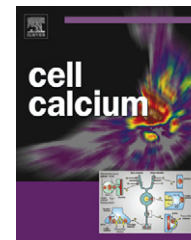




ELSEVIER

journal homepage: www.elsevier.com/locate/ceca



UVA-induced calcium oscillations in rat mast cells

Yan Dong Zhou, Xiao Feng Fang, Zong Jie Cui*

Institute of Cell Biology, Beijing Normal University, Beijing 100875, China

Received 14 December 2007; received in revised form 27 April 2008; accepted 20 May 2008

KEYWORDS

Mast cell;
UVA;
ROS;
Calcium oscillation;
NAD(P)H oxidase

Summary UVA is a major bio-active component in solar irradiation, and is shown to have immunomodulatory and anti-inflammatory effects. The detailed molecular mechanism of UVA action in regard to calcium signaling in mast cells, however, is not fully understood. In this study, it was found that UVA induced ROS formation and cytosolic calcium oscillations in individual rat mast cells. *Exogenously added H₂O₂ and hypoxanthine/xanthine oxidase (HX/XOD) mimicked UVA effects on cytosolic calcium increases.* Regular calcium oscillation induced by UVA irradiation was inhibited completely by the phosphatidylinositol-specific phospholipase C inhibitor U73122, but U73343 was without effect. Tetradrine, a calcium entry blocker, or calcium-free buffer abolished UVA-induced calcium oscillations. L-type calcium channel blocker nifedipine and stores-operated calcium channel blocker SK&F96365 had no such inhibitory effect. ROS induction by UVA was abolished after pre-incubation with anti-oxidant NAC or with NAD(P)H oxidase inhibitor DPI; such treatment also made UVA-induced calcium oscillation to disappear. UVA irradiation did not increase mast cell diameter, but it made mast cell structure more granular. Spectral confocal imaging revealed that the emission spectrum of the endogenous fluorophore in single mast cell contained a sizable peak which corresponded to that of NAD(P)H. Taken together, these data suggest that UVA in rat mast cells could activate NAD(P)H oxidase, to produce ROS, which in turn activates phospholipase C signaling, to trigger regular cytosolic calcium oscillation.

© 2008 Elsevier Ltd. All rights reserved.

Introduction

Mast cells are specialized secretory cells that synthesize and store neurotransmitters (histamine, serotonin, substance P), cytokines (IL3-6, TNF), proteases (chymase, tryptase), and others [1]. Although mast cell activation has been exten-

sively studied [2–4], it is not completely understood as to how those different mediators might be specifically or differentially released [1,5,6]. A role for calcium has long been recognized in exocytosis [7–9], but a role for calcium oscillations in mast cell secretion is not fully understood, especially in regard to specific modulation of mediator release [10–14]. Mast cell calcium oscillation has not been extensively studied other than in the mast cell/basophil cell line RBL-2H3 [15], partly due to the fact that some early works found that mast cell cytosolic calcium concentration tended not to oscillate after anti-IgE stimulation [16].

* Corresponding author. Tel.: +86 10 5880 9162;
fax: +86 10 5880 9162.

E-mail address: zjcuibnu.edu.cn (Z.J. Cui).

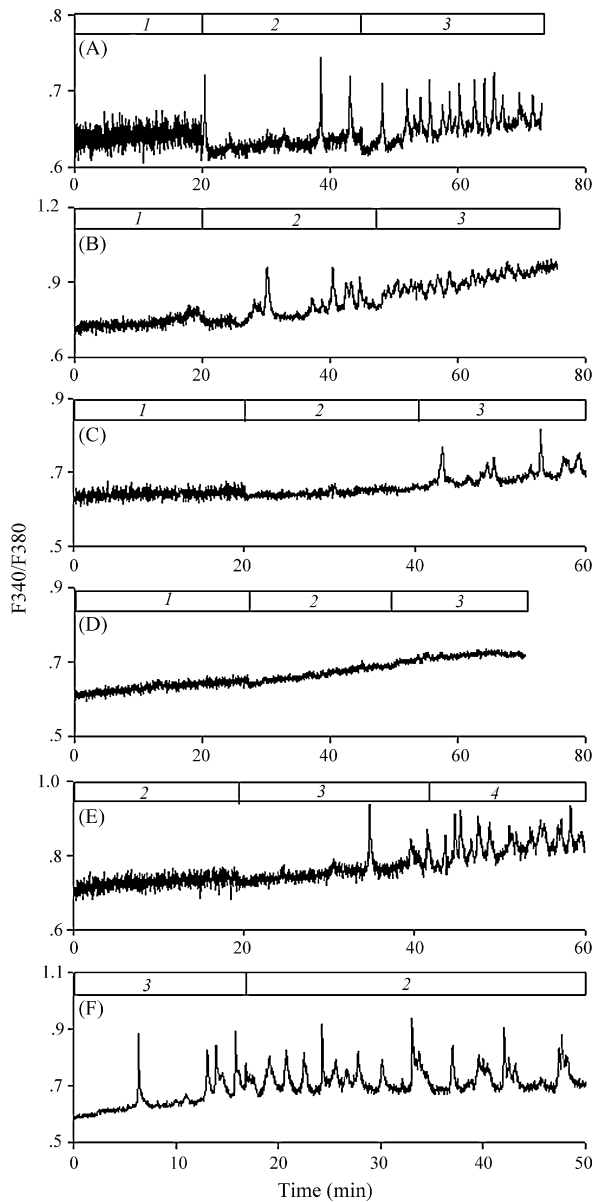


Figure 1 Light intensity-dependent induction of cytosolic calcium oscillations in isolated rat peritoneal mast cells. Fura-2-loaded-mast cells attached to Sykes-Moore chamber were perfused, and illuminated with monochromatic light from the DeltaRam V monochromator alternately at 340 nm/380 nm, the same as for normal calcium measurement. Both the in and out slits for the monochromator were initially set at a band width of 1 nm, and the resting calcium concentration remained stable at basal level. The slit width was subsequently increased as indicated (by the horizontal bars) and cytosolic calcium concentration increased in an oscillatory fashion. Traces A–D represent different response patterns observed in different mast cells. In a total of 45 experiments (only one cell could be examined in each experiment) with sequential incremental band widths from 1 to 2 to 3 nm, different response patterns were found as indicated: A: $N=7/45$; B: $N=15/45$; C: $N=19/45$; D: $N=4/45$. With sequential incremental band widths from 2 to 3 to 4 nm, all cells showed response at 4 nm (E: $N=44/44$). With sequential band widths from 3 to 2 nm, the regular calcium oscillations tended to last with a stable baseline (F: $N=11$).

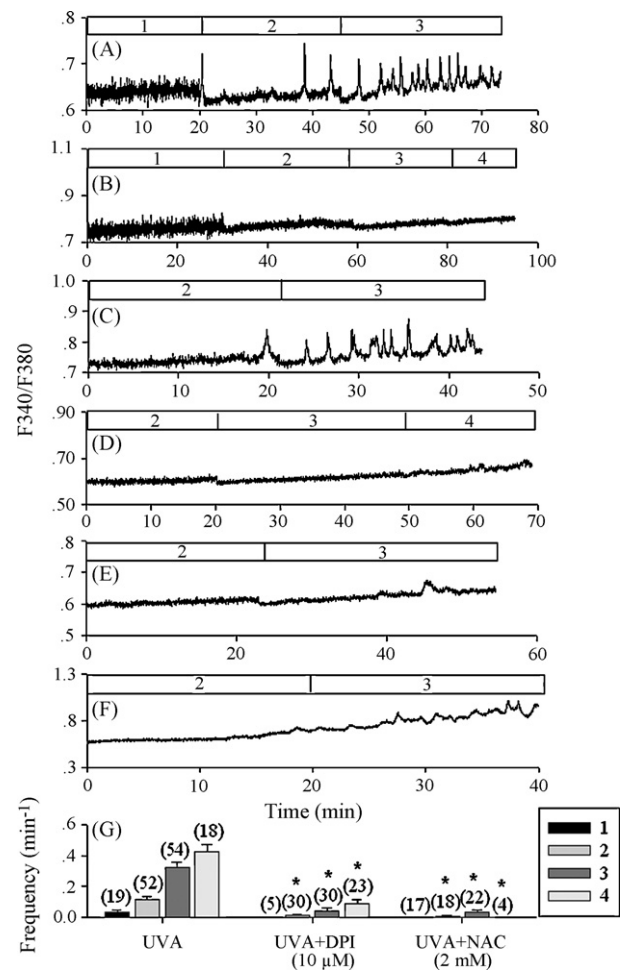


Figure 2 Antioxidant NAC and *NAD(P)H* oxidase inhibitor DPI inhibited cytosolic calcium oscillations induced by monochromatic UVA light (340 nm/380 nm). Sequential band widths from 1 to 2 to 3 nm, and from 2 to 3 nm induced regular calcium oscillations (A: $N=22$, C: $N=31$). In the presence of NAC 2 mM (B and E) or DPI 10 μM (D and F), such calcium oscillations were either completely absent even when the slit width was increased further to 4 nm (B: $N=20$, D: $N=22$), or only sparse fluctuations remained with an elevated baseline (E: $N=10$; F: $N=5$). The average oscillation frequency with UVA, UVA+NAC, and UVA+DPI at different slit width (1, 2, 3, 4 nm) was calculated and plotted in panel G. With UVA alone, the average calcium oscillation frequency (min^{-1}) at slit width of 1, 2, 3 and 4 nm was 0.033 ± 0.018 ($N=19$), 0.118 ± 0.020 ($N=52$), 0.326 ± 0.028 ($N=54$) and 0.424 ± 0.049 ($N=18$), respectively. With UVA+DPI, the average calcium oscillation frequency (min^{-1}) at slit width of 1, 2, 3 and 4 nm was 0 ($N=5$), $0.015 \pm 7.910 \times 10^{-3}$ ($N=30$), 0.041 ± 0.019 ($N=30$) and 0.087 ± 0.029 ($N=23$), respectively. With UVA+NAC, the average calcium oscillation frequency (min^{-1}) at 1, 2, 3 and 4 nm was 0 ($N=17$), $5.848 \times 10^{-3} \pm 5.848 \times 10^{-3}$ ($N=18$), 0.033 ± 0.017 ($N=22$) and 0 ($N=4$), respectively. Asterisk (*) indicates statistical significance with $P < 0.01$ when compared with UVA alone.

Oscillatory increases in intracellular calcium concentration ($[Ca^{2+}]_c$) is commonly found in *several* cell types [17], which regulate diverse cellular functions [17,18]. Oscillatory calcium concentration increases do so by frequency modulation (FM), amplitude modulation (AM), and spike shape modulation (SM), therefore encode multiple and specific signals. Lower oscillatory frequency is known to activate pro-inflammatory transcription factors NF- κ B, whereas higher frequency oscillations stimulate all three factors NF-AT, Oct/OAP and NF- κ B [18,19]. Calcium oscillations are frequently induced by endogenous physiological factors such as hormones and neurotransmitters at low, physiological concentration [18]. In the present work, we found that UVA at low doses could also trigger calcium oscillations in freshly isolated rat mast cells.

UVA is a major component of solar radiation that reaches the earth surface and is therefore a major biologically relevant UV band [20–22]. We in this work investigated the detailed mechanisms of low dose UVA-triggered cytosolic calcium oscillations. It was found that UVA (alternately at 340 and 380 nm) from the DeltaRam V monochromator of the PTI calcium measurement system readily increased intracellular ROS via activating *NAD(P)H* oxidase, which in turn induced cytosolic calcium oscillation by activating the PLC pathway. Our work is the first such report on UVA-induced *NAD(P)H* oxidase activation and ROS generation leading to calcium oscillations in mast cell, confirming UVA-induced calcium increase in other cell types such as skin keratinocytes [23].

Material and methods

Materials

SK&F96365 and tetrandrine were bought from Biomol Research Laboratories Inc. (Plymouth Meeting, PA, USA). U73122, U73343, nifedipine, diphenylene iodonium (DPI) and *N*-acetyl-cysteine (NAC), hypoxanthine, xanthine oxidase were from Sigma–Aldrich (St. Louis, MO, USA). Fura-2 AM, and 5-(and-6)-chloromethyl-2',7'-dichlorodihydrofluorescein diacetate acetyl ester (CM-H₂DCFDA) were purchased from Molecular Probes (Eugene, OR, USA). Carboxyamido-triazole (CAI) was a gift from Dr. Elise Kohn, ICR, NIH (Bethesda, MD, USA). H₂O₂ was from Beijing Chemical Engineering Factory (Beijing, China).

Isolation of rat peritoneal mast cells

Rat peritoneal mast cells were obtained as reported previously [24,25] with slight modifications. Rat of the Sprague–Dawley strain (200–400 g) was killed by cervical dislocation. Standard buffer was injected into the abdomen of the rat with a syringe. The standard buffer had the following composition (in mM): NaCl 118, KCl 4.7, CaCl₂ 2.5, MgCl₂ 1.13, NaH₂PO₄ 1, glucose 5.6, HEPES 10, glutamine 2.0, bovine serum albumin 0.2%, amino acid mixture (Gibco BRL) (50 \times), pH was adjusted to 7.4 with NaOH 4M. Buffer was oxygenated with O₂ 100% for 30 min before use. The rat abdomen was massaged for 5 min and then the abdominal cavity was opened with scissors. The ascites was centrifuged (100 \times g) for 2 \times 5 min

period. Mast cells could be readily identified by their large size and were re-suspended in standard buffer before use.

Measurement of cytosolic calcium concentration

Isolated mast cells were incubated with Fura-2 AM (final concentration 10 μ M) for 40 min at 37 °C in a shaking water bath (50 cycle min⁻¹), with oxygenation every 20 min. Fura-2 loaded-mast cells were attached to Cell-Tak coated coverslip in Sykes-Moore perfusion chamber. Attachment was allowed for 20 or 30 min before perfusion with standard buffer (without BSA and amino acid mixture), and stimulus was added by changing perfusion buffer containing relevant chemical reagents.

Sykes-Moore chamber was placed on the platform of an inverted fluorescence microscope (Olympus IX70), which was coupled to a PTI (Photon Technology International Inc., Lawrenceville, NJ, USA) microfluorometric calcium measurement system (DeltaRam V), with a photon-counting PMT (Hamamatsu PMT R1527P, i.e., PTI PMT81) as detector. Calcium concentration was indicated as fluorescence ratios F340/F380 (Figs. 1, 2 and 4–6).

A calcium imaging system (EasyRatioPro, PTI Inc., Lawrenceville, NJ, USA) was used in the detection of exogenous ROS-induced calcium increases (Fig. 3). In this imaging system, the monochromator used was DeltaRam X, inverted fluorescence microscope was Nikon TE2000U with objective Super Fluor 40 X, CCD was QuantEM 512 CS (Roper Scientific, Koto-Ku, Tokyo, Japan). Note that the fluorescence ratio (F340/F380) was higher than that obtained with the DeltaRam V (Figs. 1, 2 and 4–6).

Calcium oscillation induced by UVA irradiation

The monochromator of the PTI DeltaRam V monochromator was used as the UVA irradiation source. *UV light intensity was adjusted by changing width of the slits (both in and out) in the monochromator from 1 to 4 nm.* Basal calcium level was measured in Fura-2-loaded-mast cells with the slit-width set at 1 nm, with excitation alternating between 340 nm/380 nm and emission at >510 nm. After determining the condition of the mast cells of the day, regular calcium oscillation was induced in subsequent cells with increased slit width, which was then changed back to a smaller slit width during the measurement. For instance, if calcium oscillation was inducible at 3 nm, the slit width was set at 2 nm during measurement. Other chemicals were introduced by a change of the perfusion buffer containing the relevant chemicals. The UVA irradiance at each slit width was measured by an IL 1700 research radiometer (International Light Inc., Newburyport, MA01950, USA), and shown in Table 1.

Measurement of intracellular reactive oxygen species (ROS)

Intracellular ROS production was measured with ROS indicator CM-H₂DCFDA. In order to avoid artifacts, the loading of CM-H₂DCFDA was performed after UVA irradiation, as

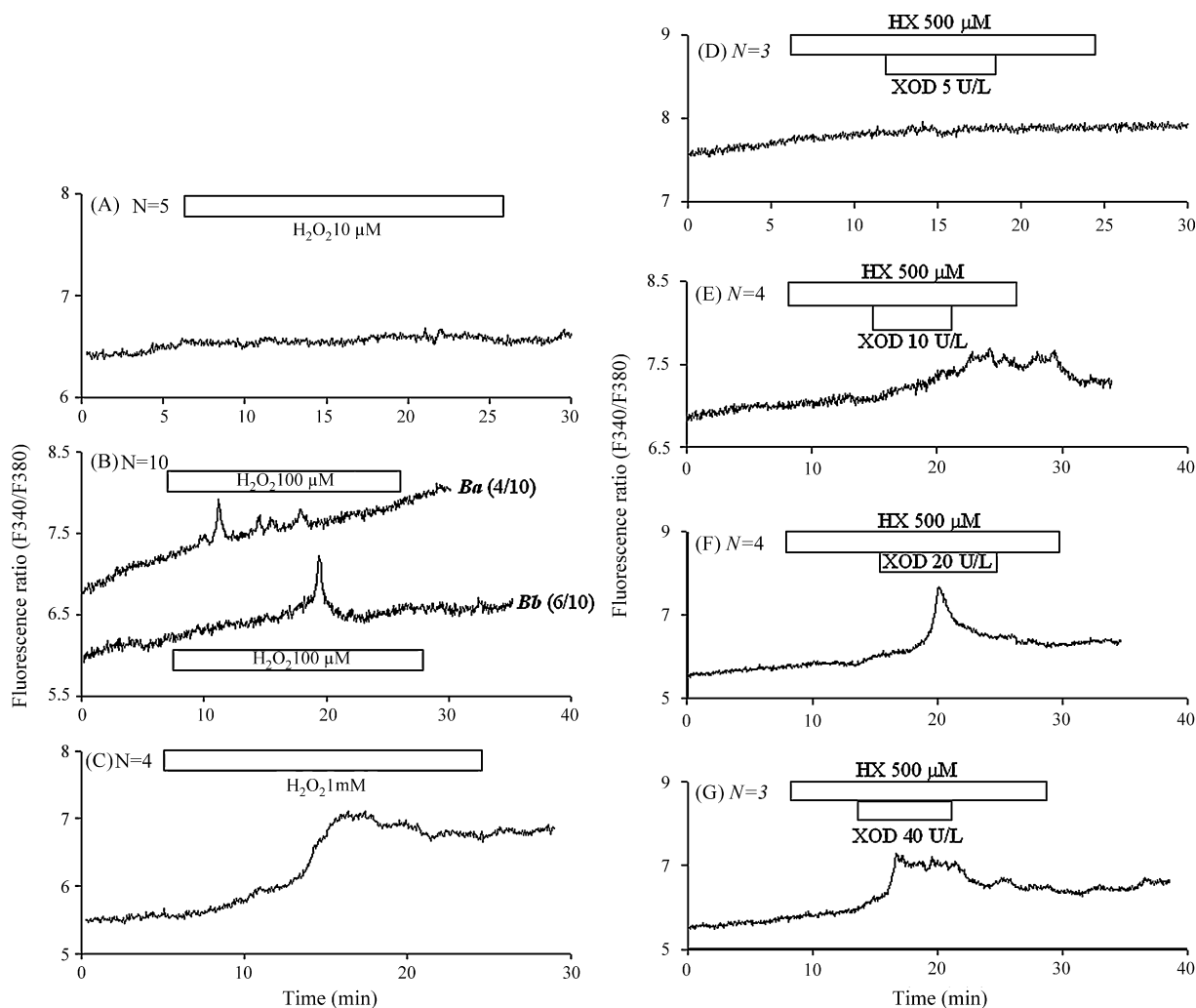


Figure 3 H_2O_2 and HX/XOD mimicked UVA effects on cytosolic calcium concentration. Freshly isolated rat peritoneal mast cells were stimulated with H_2O_2 or HX/XOD as indicated in A–G. A–C: Perfused Fura-2-loaded peritoneal mast cells were stimulated with H_2O_2 at 10 (A), 100 (B) and 1000 μM (C). D–G: Mast cells were perfused with hypoxanthine (HX) 500 μM , together with xanthine oxidase (XOD) of 5 (D), 10 (E), 20 (F), 40 (G) U/L^{-1} . Drugs were added as indicated by the horizontal bars. The N numbers mean each calcium trace is representative of N separate experiments: A, $N=5$; B, $N=10$ (Ba, $N=4$; Bb, $N=6$); C, $N=4$; D, $N=3$; E, $N=4$; F, $N=4$; G, $N=3$.

Table 1 UVA irradiance from PTI DeltaRam V at alternating 340 nm/380 nm with different slit width ($\times 10^{-7} \text{W cm}^{-2}$)

Slit width (nm)	Irradiance ($\times 10^{-7} \text{W cm}^{-2}$)
1	3.02 ± 0.11
2	12.56 ± 0.36
3	28.92 ± 0.81
4	51.91 ± 1.17
5	79.45 ± 1.79
6	111.74 ± 2.32
8	193.98 ± 4.33

The sensor of an IL 1700 research radiometer was placed on the IX70 Olympus microscope platform at a position similar to mast cells in the Sykes-Moore chamber, a stable reading was recorded on 10 separate occasions at each slit width from 1 to 8 nm. Data are presented as mean \pm S.E.M.

cautioned by others [26]. Cells were attached to Cell-Tak treated cover-slip in the Sykes-Moore perfusion chamber and treated as described above to obtain regular calcium oscillation. Mast cells were incubated with CM- H_2DCFDA (4 μM) for 30 min immediately after UVA treatment. CM- H_2DCFDA fluoresces after oxidization in the cytoplasm. CM- H_2DCFDA -loaded cells were perfused, fluorescence (F_s) in a single mast cell was read at λ_{ex} 490 nm and λ_{em} 525 nm for 30 s continuously. Background fluorescence (F_b) was read under the same condition. Relative ROS level in single mast cell was expressed as F_s/F_b . The fluorescence in this series of experiments was measured in the PTI DeltaRam V system.

Confocal imaging and emission spectrum of single mast cells

The emission spectrum of the endogenous fluorophore in single mast cells was determined in a spectral confocal

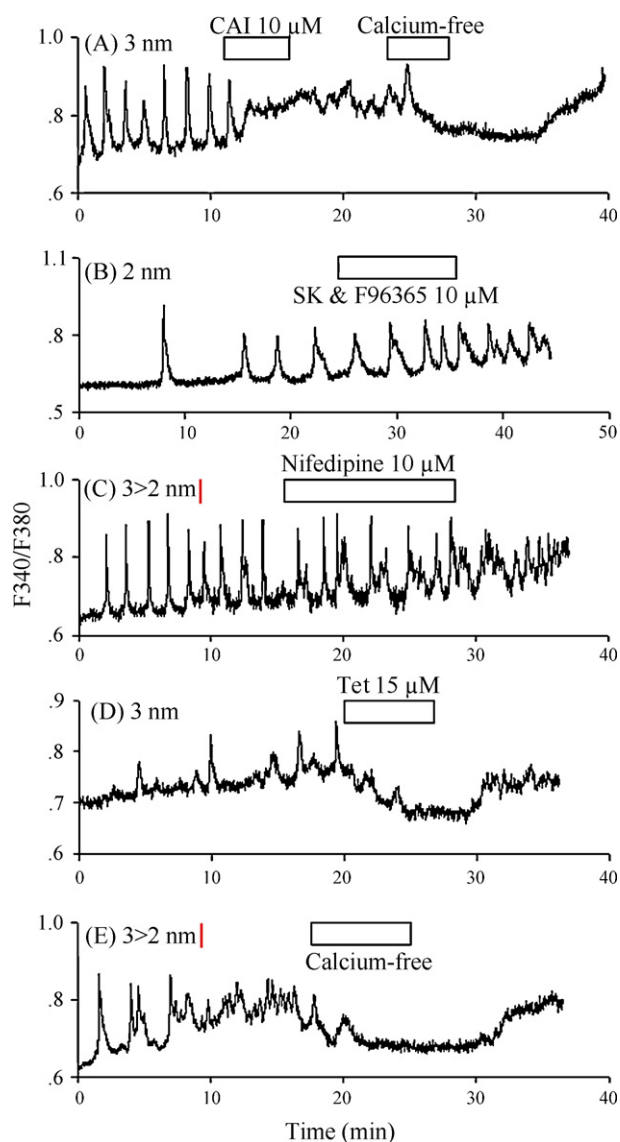


Figure 4 Effects of modulating calcium entry on UVA-induced calcium oscillations in mast cells. Regular calcium oscillations were induced individually for each mast cell. Effects of CAI 10 μM , SK&F96365 (10 μM), nifedipine 10 μM , tetrandrine 15 μM and calcium-free buffer on UVA-induced calcium oscillations in mast cells were shown. Each trace in panels A–E is representative of N independent experiments: A, $N=3$; B, $N=8$; C, $N=9$; D, $N=10$; E, $N=3$. All drugs were added as indicated by the horizontal bars. The slit width was 3 nm throughout the experiment in panels A and D, 2 nm for panel B; the slit width was changed from 3 to 2 nm at time indicated by the vertical line in panels C and E.

microscope (Leica TCS Sp2 plus Leica DMIR) with objective 40 \times (N.A. 1.25) equipped with a UV excitation lamp. Isolated mast cells adhered to Cell-Tak-coated cover-slip was excited at λ_{ex} 364 nm (band width 360–380 nm), and emission scanned from 400 to 600 nm. Subsequently the fluorescence images were taken at λ_{ex} 364 nm and λ_{em} 433 nm.

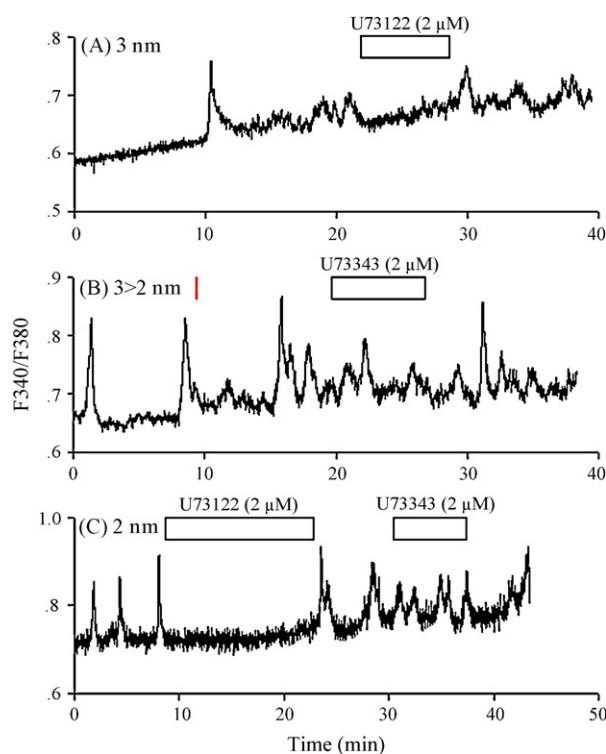


Figure 5 Role of phospholipase C in UVA-induced cytosolic calcium oscillations in rat mast cells. Regular calcium oscillations were induced individually for each mast cell. Effects of phospholipase C inhibitor U73122 (2 μM), and inactive analogue U73343 (2 μM) were investigated separately in different mast cells (A and B) or in the same cell (C), drug addition was as indicated by the horizontal bars. Each trace in panels A–C is representative of N similar experiments: A, $N=25$; B, $N=15$; C, $N=3$. The slit width was 3 nm in panel A, and 2 nm in panel C; the slit width was changed from 3 to 2 nm at time indicated by the vertical line in panel B.

Statistical analysis

Each experiment reported in this work has been done at least three times on different days with different animals. Data are expressed as mean \pm S.E.M. Figures were plotted by SigmaPlot. To examine the differences between different experimental groups, Student's T test was used, with $P < 0.05$ taken as statistically significant.

Results

UVA-induced regular calcium oscillations in rat mast cells

To determine UVA effects on cytosolic calcium concentration, Fura-2-loaded-mast cells attached to Cell-Tak-coated cover-slips were excited with alternating light of 340 and 380 nm. In most experiments excitation light was delivered from the DeltaRam V monochromator with both in and out slips set at 1 nm (i.e., band width of 1 nm). With this setting, basal calcium concentration remained stable. When the slit width was increased, regular calcium

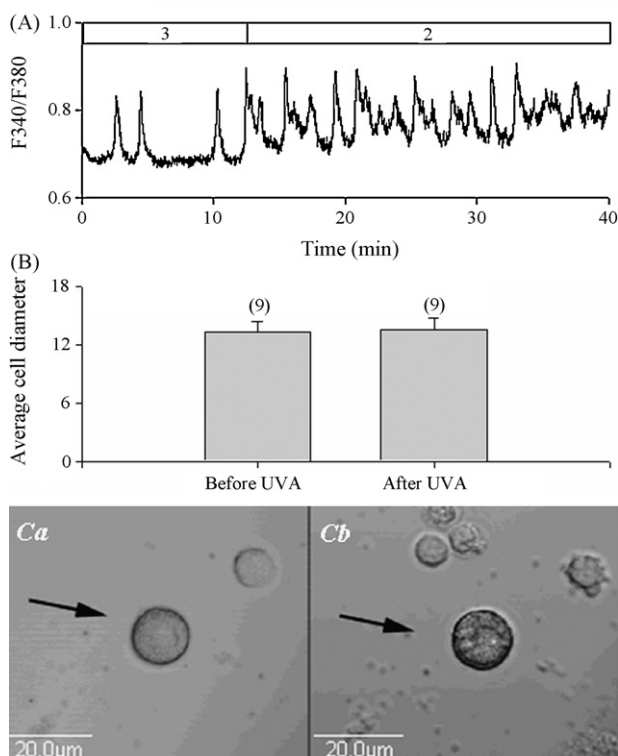


Figure 6 Morphological changes induced by UVA in rat mast cells. Regular calcium oscillations were induced in mast cells similar to Fig. 1F and as indicated in panel A, the slit width being indicated by the horizontal bars. Mast cell images were taken both before and after calcium measurement, and cell diameters (in μm) were compared. Mast cell diameter was measured with the ruler tool in Photoshop (B). Panel C shows mast cell morphological changes in a typical experiment. The arrows in Ca and Cb indicate the mast cell used for both calcium and diameter measurements. Panels A and C are representative of 9 independent experiments. DIC images were taken in the scanning mode in an Olympus IX 71 microscope coupled to the FV300 laser scanning unit, with objective $\times 40$ (N.A. 1.25).

oscillations appeared. Fig. 1A–D show 4 typical responses in cytosolic calcium concentration increases. The differences in responses in individual cells were obviously due to mast cell heterogeneity reported previously also by others [27]. Regular calcium oscillations were induced with the slit width at 2 nm (Fig. 1A and B), or 3 nm (Fig. 1C), with a minor number showing no oscillation even at 3 nm (Fig. 1D, 4/45). When the initial slit width was set at 2 nm, most cells started to show calcium oscillations when the slit width was increased to 3 nm. In Fig. 1D, a slow phasic increase in cytosolic calcium was found; this could be due to slow activation of a nonselective cationic current permeable to calcium as reported by others [28]. With a starting slit width of 3 nm, calcium oscillation was readily observed (Fig. 1E), and once calcium oscillation was induced, oscillation could be maintained at a lower slit width (Fig. 1F). It may be noted here that UVA irradiances at different slit width was measured and presented in Table 1. The average UVA dosage with alternating wavelength of 340 nm/380 nm used in this work was in the range

of $3.02\text{--}51.91 \times 10^{-7} \text{ W cm}^{-2}$, corresponding to slit width of 1–4 nm.

A role for ROS in UVA-induced calcium oscillations in mast cells

UVA irradiation indeed induced regular calcium oscillations. To determine the possible mechanisms involved, Fura-2-loaded-mast cells were treated with standard buffer, with ROS scavengers NAC (2 mM), or with *NAD(P)H* oxidase inhibitor DPI (10 μM) for 1 h before UVA irradiation. As shown in Fig. 2A and C, mast cells without any pre-treatment showed regular calcium oscillations with UVA irradiation; whereas after incubation with NAC (Fig. 2B and E) or DPI (Fig. 2D and F), calcium oscillations completely disappeared when UVA irradiated. UVA alone induced regular calcium oscillations in 89% of the mast cells examined (41 of 46). In the presence of NAC and DPI, no oscillations were observed, but a slow increase was found in 14% (3 of 21), and 22% (6 of 27) cell examined, respectively (Fig. 2E and F). The average oscillatory frequency at 1–4 nm, under different conditions were analyzed and presented in Fig. 2G. It was obvious that both DPI and NAC markedly blocked UVA-induced calcium oscillations. From these data, it was obvious that intracellular ROS was essential for UVA induction of calcium oscillations.

To corroborate further a role for ROS in UVA-induced increases in cytosolic calcium concentration, effects of exogenous ROS was examined. H_2O_2 and hypoxanthine/xanthine oxidase (HX/XOD) system were used to mimic effects of superoxide anion. It was found that H_2O_2 induced dose-dependent increases in cytosolic calcium concentration. H_2O_2 at 10 μM was without any obvious effect, but at 100 μM induced sparse or recurrent calcium spikes, and at 1000 μM induced a plateau increase (Fig 3.1). Similarly, the HX/XOD system also induced readily cytosolic calcium concentration increases. In control experiments it was found that HX (500 μM) alone had no effect. HX (500 μM) plus XOD induced increases in cytosolic calcium concentration dependent on the concentration of XOD. HX plus XOD at 5 UL^{-1} induced no obvious increase, at 10 UL^{-1} induced fluctuations in cytosolic calcium concentration, at 20 and 40 UL^{-1} induced a phasic increase with a much broader peak at 40 than at 20 UL^{-1} (Fig. 3.2). Therefore both H_2O_2 and the HX/XOD system induced fluctuatory increases in cytosolic calcium concentration in peritoneal mast cells, mimicking the effects of UVA irradiation.

A role for calcium influx in UVA-induced calcium oscillations in mast cells

Other than intracellular ROS, it was found that calcium influx was needed for UVA-induced calcium oscillations to persist. In this series of experiments, regular calcium oscillations were induced with large slit width (2–3 nm); then oscillations were maintained at lower slit numbers. The calcium influx blocker carboxyamido-triazole [29] at 10 μM was able to disrupt regular calcium oscillations, subsequent removal of extracellular calcium completely reduced calcium concentration to the basal level (Fig. 4A). On the other hand, both SK&F96365 [30] (Fig. 4B) and nifedipine

were without any effect on UVA-induced calcium oscillations (Fig. 4C). Tetrandrine 15 μM , an active ingredient from Chinese medicine and a calcium channel antagonist, effectively reduced UVA-induced oscillatory calcium increase to below the basal level (Fig. 4D). Removal of extracellular calcium effectively blocked UVA-induced oscillatory calcium increases (Fig. 4E). These data suggest that the presence of external calcium was needed for UVA-induced calcium oscillation to persist in mast cells.

Involvement of phospholipase C in UVA-induced calcium oscillations in mast cells

To assess the critical source of calcium oscillation for UVA irradiation-induced calcium oscillations, U73122, a phospholipase C inhibitor, was used. U73122 at 2 μM completely abolished UVA-induced calcium oscillations in mast cell (Fig. 5A and B), whereas the structural analogue U73343 at 2 μM was without any effect (Fig. 5B and C), both in different cells (Fig. 5A and B) and in the same mast cell (Fig. 5C). These data indicate that like *neurotransmitter*- or *hormone*-induced calcium oscillations in glandular and liver cells [31–33], UVA-induced calcium oscillation is also mediated by the PI-PLC signaling pathway. Further, UVA irradiation-induced PLC-activation was reversible.

To assess the extent of mast cell activation by UVA irradiation, mast cells were imaged by laser confocal microscopy both before and after UVA treatment and calcium measurement. Mast cell was first imaged before UVA irradiation (Fig. 6Ca), then calcium oscillations were induced with UVA (Fig. 6A); 40 min later, the same mast cell was imaged again (Fig. 6Cb). The average diameter of mast cells both before and after UVA irradiation did not show any significant change (Fig. 6B). Although the average cell diameter did not change, mast cells underwent a major structural change after UVA irradiation (cf. Fig. 6Ca and Cb); a granular texture was found in UVA-irradiated cells, although no obvious exosomes were detected.

UVA irradiation-induced intracellular ROS generation in single mast cells

It has been reported before that UV irradiation generates intracellular ROS in non-phagocytic cells such as human keratinocytes [23,34]. To confirm a role for ROS in UVA-induced calcium oscillations, the actual generation of ROS after UVA irradiation was measured with the ROS probe CM-H₂DCFDA. CM-H₂DCFDA when oxidized by ROS inside the cell to DCF, shows a significant increase in fluorescence. To avoid direct effects of UVA irradiation on CM-H₂DCFDA, in our experiments, mast cells were first UVA irradiated as above, then UVA-irradiated mast cells were loaded with the ROS probe CM-H₂DCFDA. The difference in DCF fluorescence was taken as an indicator of ROS generation. As shown in Fig. 7, the relative ROS in control mast cells not treated with UVA was about 1.232 ± 0.154 , after UVA irradiation, the relative ROS increased to 3.092 ± 0.875 . Notably, when mast cells were pre-treated with ROS scavenger NAC (2 mM), UVA-induced ROS was inhibited markedly (Fig. 7A and B).

Pre-treatment of mast cells with *NAD(P)H* oxidase inhibitor DPI for 1 h prior to UVA light, completely abol-

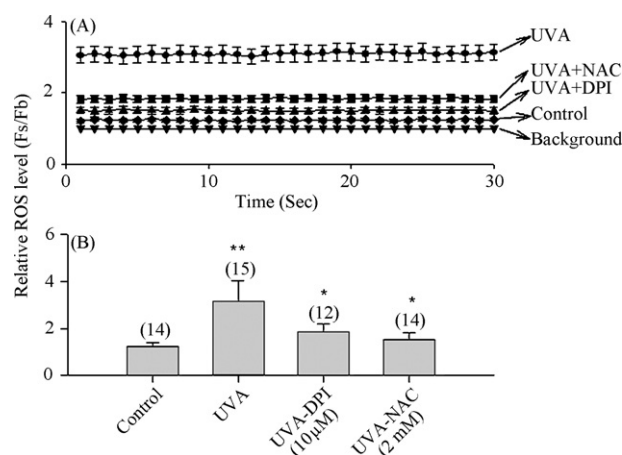


Figure 7 UVA-induced ROS generation and its inhibition by antioxidants NAC and *NAD(P)H* oxidase inhibitor DPI. In these experiments, mast cells were exposed to UVA as shown in Fig. 1A. After UVA irradiation mast cells were immediately incubated with CM-H₂DCFDA at 4 μM for 30 min at room temperature. Fluorescence was then measured, with the monochromator slit-width set at 1 nm. Control cells were not previously exposed to UVA. For NAC and DPI groups, NAC 2 mM and DPI 10 μM was added to adherent mast cells 1 h before UVA irradiation. DCFDA fluorescence was monitored for 30 s after such treatments, and expressed as fluorescence ratio Fs/Fb, Fs being mast cell fluorescence, Fb being background fluorescence of blank region of the same size. Panel A plots real time measurement, Panel B plots averaged ROS generation over 30 s in mean \pm S.E.M. Control, $N = 14$; UVA, $N = 15$; UVA + DPI, $N = 12$; UVA + NAC, $N = 14$. The asterisks (**) denotes $P < 0.001$ compared with control, and (*) denotes $P < 0.01$, compared with UVA alone.

ished UVA-induced ROS generation. The relative ROS level in UVA + DPI, and UVA + NAC groups was 1.834 ± 0.340 , and 1.504 ± 0.316 , respectively. These results suggest that *NAD(P)H* oxidase was involved in UVA-induced ROS generation and calcium oscillations.

Subcellular localization and spectral features of the endogenous chromophore

To identify the potential molecular target for UVA action that led to cytosolic calcium oscillations, an emission spectrum of endogenous chromophores were obtained. Excitation at 360–380 nm induced ready fluorescence in mast cells (Fig. 8). With the Leica SP2, it was possible to determine the emission spectrum (Fig. 8A). A major emission peak was found at 434 nm, with 3 minor peaks at longer wavelengths. With λ_{ex} 364 nm and λ_{em} 434 nm, it was possible to image the endogenous chromophores. At the molecular level, various chromophores have been identified, and DNA remains the major chromophore. It was obvious that the major chromophores *here* were located in the cytosol instead of the nucleus (Fig. 8B). Further, the major chromophore responded to UVA in rat peritoneal mast cells is not DNA (Fig. 8). In the experiments measuring $[\text{Ca}^{2+}]_c$ oscillation and intracellular ROS, mast cells were irradiated by UVA of 340 and 380 nm wavelength. In a Leica confocal SP2, mast cell fluorescence image was taken with λ_{ex} from 360

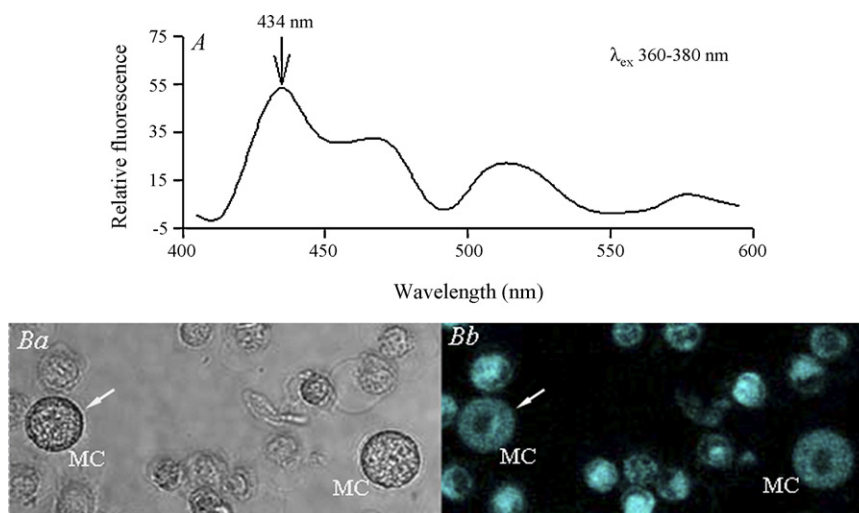


Figure 8 Subcellular localization and spectral features of the UVA responsive endogenous chromophore in rat mast cells. Freshly isolated rat mast cells were imaged in a Leica confocal microscope (TCS Sp2 plus DMIR) (ocular 10 \times , objective 40 \times , N.A. 1.25). A: Emission spectrum of a single mast cell (indicated by the arrow in Ba and Bb). Excitation light was through a band-pass filter (360–380 nm) with maximum transmission at 364 nm; emission was measured from 400 to 600 nm. Maximum emission was found to be at 434 nm. Ba and Bb are bright field and fluorescent images of examined mast cells (MC). Fluorescent image in Bb was taken with λ_{em} at 434 nm. Note the cytosolic localization of the endogenous chromophore.

to 380 nm. The image clearly indicated that the endogenous fluorophore was mainly cytosolic (Fig. 8B). So the possible target of UVA action in mast cell is unlikely to be genomic DNA. With λ_{ex} set at 360–380 nm, a λ_{em} maximum was found at 433 nm, with 3 smaller peaks at longer wavelengths (Fig. 8A). The implications of such data are discussed later in the ‘Discussions’.

Discussions

Both ultraviolet A (320–400 nm) and ultraviolet B (290–320 nm) are major solar UV components that could reach the torrential surface, and therefore are the most biologically relevant. UVA has both immunomodulatory [35–37] and immunoprotective effects [38,39]. Such effects may be related to UVA modulation of mast cells.

A bimodal effect of UVA on mast cells has been established early on: with exogenous photosensitizer present, low level UVA irradiation inhibited mast cell secretion, whereas high doses resulted in a stimulation of mast cell mediator release [40]. UVA irradiation alone triggers histamine release from mast cells, and leads to marked suppression of anti-IgE-induced histamine release [41]. *It may be noted here that low UV light has been shown to reduce angiotensin-induced cytosolic calcium increase in adrenal glomerulosa cells, although it had no effect on basal calcium levels* [42]. Those early studies notwithstanding, it is nevertheless not known in detail how UVA might affect the calcium signaling pathway in mast cells.

ROS are known to play an important role in mast cell activation and degranulation [34,43]. Stimulated rat mast cells release ROS [44,45]. Some authors argued that mast cell ROS production could be due to contaminating macrophages [46,47]. In the present study, ROS generation was directly measured in single rat mast cell microscopically, therefore

directly confirming mast cell generation of ROS. *The fact that exogenous ROS (H_2O_2 and HX/XOD) mimicked UVA-induced calcium increases (Fig. 3) confirms a role for ROS in UVA activation of mast cells.*

Low level ($(12-51) \times 10^{-7} \text{ W cm}^{-2}$) UVA directly activated ROS production, which was nearly completely blocked by NAD(P)H oxidase inhibitor DPI (Fig. 7), implicating NAD(P)H oxidase as a source of ROS production. The ROS quencher NAC completely blocked CM- H_2 DCFDA oxidation and associated fluorescence increase, further confirming the role for NAD(P)H oxidase. Most importantly, both NAC and DPI significantly blocked UVA-induced calcium oscillations (Fig. 2), suggesting an essential role for NAD(P)H oxidase-derived ROS in triggeration of mast cell cytosolic calcium oscillation. How cytosolic ROS might activate calcium oscillations is not known at the moment. But it is firmly established in the present work that PLC-activation is essential (Fig. 5).

Early work found that UVA irradiation led to the activation of a novel calcium-permeable cationic current in mast cells [28]. Calcium influx was also found to be important for the maintenance of UVA-induced calcium oscillations in this work (Fig. 4). But the calcium influx involved was not susceptible to known inhibitors of L-type voltage-dependent calcium channel inhibitor nifedipine or stores-operated calcium channel inhibitor SK&F 96365 (Fig. 4). Rather, the UVA-activated calcium influx was blocked by tetrandrine (Fig. 4D), an active component from the root of *Stephania tetrandra* S Moore. Tetrandrine as a wide-spectrum calcium antagonist effective towards both voltage-dependent and voltage-independent calcium channels has been widely recognized [48–51], although it may also have other effects, such as inhibition of IP_3 production and of other ion channels [52–54]. Tetrandrine in this work may have blocked UVA-induced calcium oscillation due to a combination of all these effects.

UVA-induced calcium oscillations were not accompanied by obvious changes in mast cell size, although major structural changes were readily observed; the mast cell after UVA became more granular which suggested secretion (Fig. 6). It could be concluded that low level UVA in the range of $(1.2\text{--}5.1) \times 10^{-6} \text{ W cm}^{-2}$ was able to induce both calcium oscillation and possibly mast cell secretory response. The endogenous chromophore responsible was not identified at this moment, but it had a major emission peak at 434nm and several smaller peaks at longer wavelengths. The chromophore was located mainly in cytosol (Fig. 8). The potential candidates at longer emission peaks may include NADH/NAD(P)H [55], and riboflavin [56–58], which would correspond to the smaller emission peaks at 470 and 520 nm, respectively (see Fig. 8A and [59,60]). Work by others has suggested that proteins and lipids near or in the plasma membrane may also be involved [61].

It may be noted here that it is not completely clear how phospholipase C was activated by UVA-induced ROS. But UVA irradiation has been shown to inactivate membrane-associated protein tyrosine phosphatase (PTP) by: (i) cysteine oxidation in the active center of PTP [62], or (ii) oxidation changing PTP conformation [63]. We have previously shown that singlet oxygen could modulate plasma membrane protein secondary structure [64]. ROS produced by NAD(P)H oxidase could therefore activate phospholipase C by direct oxidation of relevant amino acid residues at the reactive center, or by modulation of other residues which change the 3-D conformation of phospholipase C and leads to its activation or increased activity.

Fig. 6C as noted above suggests that UVA could possibly have induced mast cell secretion, the mast cell structure becoming more granular. This would possibly imply a physiological role for low dose UVA in mast cell biology. Mast cells after IgE stimulation are known previously to produce functionally significant amount of ROS but no nitric oxide [47]. NAD(P)H oxidase-mediated ROS production and subsequent induction of calcium oscillations reported in the present work may contribute to mast cell cytokine production, as reported before in other cell types [34]. A recent report found that high affinity IgE receptor activation induced ROS generation was completely abolished with 5-lipoxygenase inhibitors, but not with NAD(P)H oxidase inhibitor DPI. When IgE receptor-mediated ROS generation was blocked, mast cell degranulation and cytokine production remained un-affected in those human mast cells (huMC) and mouse bone marrow-derived mast cells (mBMMC), further implicating NAD(P)H oxidase-mediated ROS production in mast cell degranulation and cytokine production [65], i.e., different sources of ROS may produce different end effects. This is further confirmed in the present study in that exogenously added ROS by H_2O_2 and HX/XOD only MIMICKED UVA-induced calcium increase; regular calcium oscillations seen with UVA were not readily detected with exogenous ROS (Fig. 3). IgE and UVA induce different sources of ROS production and therefore differential release of mast cell mediators would make perfect sense.

In conclusion, the above data together suggest that UVA irradiation may sequentially activate NAD(P)H oxidase, to produce ROS, which in turn activate phospholipase C, to induce calcium oscillations in mast cells. The fact that UVA induces oscillatory increases in cytosolic calcium concentra-

tion suggests that UVA may encode multiple signals therefore be involved in the modulation of multiple and specific mast cell functions, or UVA may modulate the release of specific secretory mediators.

Conflicts of interest

We hereby declare that there is no conflict of interest in the work contained in the above MS.

Acknowledgments

This work was supported by grants from NSF China (Nos. 30472048, 3054042524 and 30728020) and from NSF Beijing (No. 6062014).

References

- [1] T.C. Theoharides, D. Kempuraj, M. Tagen, P. Conti, D. Kalogeromitros, Differential release of mast cell mediators and the pathogenesis of inflammation, *Immunol. Rev.* 217 (2007) 65–78.
- [2] T. Oka, K. Sato, M. Hori, H. Ozaki, H. Karaki, FcepsilonRI cross-linking-induced actin assembly mediates calcium signalling in RBL-2H3 mast cells, *Br. J. Pharmacol.* 136 (2002) 837–846.
- [3] Y. Suzuki, T. Yoshimaru, T. Matsui, T. Inoue, O. Niide, S. Nunomura, C. Ra, Fc epsilon RI signaling of mast cells activates intracellular production of hydrogen peroxide: role in the regulation of calcium signals, *J. Immunol.* 171 (2003) 6119–6127.
- [4] S. Yamasaki, T. Saito, Regulation of mast cell activation through FcepsilonRI, *Chem. Immunol. Allergy* 87 (2005) 22–31.
- [5] M. Triggiani, G. Giannattasio, B. Balestrieri, F. Granata, M.H. Gelb, A. de Paulis, G. Marone, Differential modulation of mediator release from human basophils and mast cells by mizolastine, *Clin. Exp. Allergy* 34 (2004) 241–249.
- [6] M. Wu, T. Baumgart, S. Hammond, D. Holowka, B. Baird, Differential targeting of secretory lysosomes and recycling endosomes in mast cells revealed by patterned antigen arrays, *J. Cell Sci.* 120 (2007) 3147–3154.
- [7] E.R. Chapman, Synaptotagmin: a Ca^{2+} sensor that triggers exocytosis? *Nat. Rev. Mol. Cell Biol.* 3 (2002) 498–508.
- [8] J.W. Barclay, A. Morgan, R.D. Burgoyne, Calcium-dependent regulation of exocytosis, *Cell Calcium* 38 (2005) 343–353.
- [9] A.G. Garcia, A.M. Garcia-De-Diego, L. Gandia, R. Borges, J. Garcia-Sancho, Calcium signaling and exocytosis in adrenal chromaffin cells, *Physiol. Rev.* 86 (2006) 1093–1131.
- [10] Y. Nakata, I. Hide, Calcium signaling and protein kinase C for TNF- α secretion in a rat mast cell line, *Life Sci.* 62 (1998) 1653–1657.
- [11] D. Baram, M. Linial, Y.A. Mekori, R. Sagi-Eisenberg, Ca^{2+} -dependent exocytosis in mast cells is stimulated by the Ca^{2+} sensor, synaptotagmin I, *J. Immunol.* 161 (1998) 5120–5123.
- [12] D. Baram, R. Adachi, O. Medalia, M. Tuvim, B.F. Dickey, Y.A. Mekori, R. Sagi-Eisenberg, Synaptotagmin II negatively regulates Ca^{2+} -triggered exocytosis of lysosomes in mast cells, *J. Exp. Med.* 189 (1999) 1649–1658.
- [13] D. Baram, Y.A. Mekori, R. Sagi-Eisenberg, Synaptotagmin regulates mast cell functions, *Immunol. Rev.* 179 (2001) 25–34.
- [14] R. Sagi-Eisenberg, The mast cell: where endocytosis and regulated exocytosis meet, *Immunol. Rev.* 217 (2007) 292–303.
- [15] M. de Bernard, A. Cappon, L. Pancullo, RuggieroP, RiveraJ, G.D. Giudice, C. Montecucco, The *Helicobacter pylori* VacA cytotoxin activates RBL-2H3 cells by inducing cytosolic calcium oscillations, *Cell Microbiol.* 7 (2005) 191–198.

- [16] D. MacGlashan Jr., C.B. Guo, Oscillations in free cytosolic calcium during IgE-mediated stimulation distinguish human basophils from human mast cells, *J. Immunol.* 147 (1991) 2259–2269.
- [17] G. Dupont, L. Combettes, L. Leybaert, Calcium dynamics: spatio-temporal organization from the subcellular to the organ level, *Int. Rev. Cytol.* 261 (2007) 193–245.
- [18] L. Su, C.Y. Ma, Y.D. Zhou, Y.H. Jia, Z.J. Cui, Cytosolic calcium oscillations in the submandibular gland cells, *Acta Pharmacol. Sin.* 27 (2006) 843–847.
- [19] R.E. Dolmetsch, K. Xu, R.S. Lewis, Calcium oscillations increase the efficiency and specificity of gene expression, *Nature* 392 (1998) 933–936.
- [20] B.L. Diffey, Sources and measurement of ultraviolet radiation, *Methods* 28 (2002) 4–13.
- [21] P. Grof, G. Ronto, E. Sage, A computational study of physical and biological characterization of common UV sources and filters, and their relevance for substituting sunlight, *J. Photochem. Photobiol. B-Biol.* 68 (2002) 53–59.
- [22] S. Seite, C. Medaiko, F. Christiaens, C. Bredoux, D. Compaan, H. Zucchi, D. Lombard, A. Fourtanier, Biological effects of simulated ultraviolet daylight: a new approach to investigate daily photoprotection, *Photodermatol. Photoimmunol. Photomed.* 22 (2006) 67–77.
- [23] A. Valencia, I.E. Kochevar, Nox1-based NAD(P)H oxidase is the major source of UVA-induced reactive oxygen species in human keratinocytes, *J. Invest. Dermatol.* 128 (July) (2007) 214–222.
- [24] R. Penner, M. Pusch, E. Neher, Washout phenomena in dialyzed mast cells allow discrimination of different steps in stimulus-secretion coupling, *Biosci. Rep.* 7 (1987) 313–321.
- [25] S. Hashikura, Y. Satoh, Z.J. Cui, Y. Habara, Photodynamic action inhibits compound 48/80-induced exocytosis in rat peritoneal mast cells, *Jpn. J. Vet. Res.* 49 (2001) 239–247.
- [26] C.F. Chignell, R.H. Sik, A photochemical study of cells loaded with 2',7'-dichlorofluorescein: implications for the detection of reactive oxygen species generated during UVA irradiation, *Free Radic. Biol. Med.* 34 (2003) 1029–1034.
- [27] L.C. Yong, The mast cell: origin, morphology, distribution, and function, *Exp. Toxicol. Pathol.* 49 (1997) 409–424.
- [28] F. Mendez, R. Penner, Near-visible ultraviolet light induces a novel ubiquitous calcium-permeable cation current in mammalian cell lines, *J. Physiol.* 507 (1998) 365–377.
- [29] A. Enfissi, S. Prigent, P. Colosetti, T. Capiod, The blocking of capacitative calcium entry by 2-aminoethyl diphenylborate (2-APB) and carboxyamidotriazole (CAI) inhibits proliferation in Hep G2 and Huh-7 human hepatoma cells, *Cell Calcium* 36 (2004) 459–467.
- [30] J.E. Merritt, W.P. Armstrong, C.D. Benham, T.J. Hallam, R. Jacob, A. Jaxa-Chamiec, B.K. Leigh, S.A. McCarthy, K.E. Moores, T.J. Rink, SK&F 96365, a novel inhibitor of receptor-mediated calcium entry, *Biochem. J.* 271 (1990) 515–522.
- [31] Z.J. Cui, Y. Habara, Y. Satoh, Photodynamic modulation of adrenergic receptors in the isolated rat hepatocytes, *Biochem. Biophys. Res. Commun.* 277 (2000) 705–710.
- [32] Y.P. An, R. Xiao, H. Cui, Z.J. Cui, Selective activation by photodynamic action of cholecystokininreceptor in the freshly isolated rat pancreatic acini, *Br. J. Pharmacol.* 139 (2003) 872–880.
- [33] R. Xiao, Z.J. Cui, Mutual dependence of VIP/PACAP and CCK receptor signaling for a physiological role in duck exocrine pancreatic secretion, *Am. J. Physiol.* 286 (2004) R189–198.
- [34] Y. Suzuki, T. Yoshimaru, T. Inoue, O. Niide, C. Ra, Role of oxidants in mast cell activation, *Chem. Immunol. Allergy* 87 (2005) 32–42.
- [35] J. Krutmann, A. Morita, Mechanisms of ultraviolet (UV) B and UVA phototherapy, *J. Invest. Dermatol. Symp. Proc.* 4 (1999) 70–72.
- [36] M. El-Mofty, W. Mostafa, S. Esmat, R. Youssef, M. Bousseila, N. Nagi, O. Shaker, A. Abouzeid, Suggested mechanisms of action of UVA phototherapy in morphea: a molecular study, *Photodermatol. Photoimmunol. Photomed.* 20 (2004) 93–100.
- [37] P.H. Hart, S.L. Townley, M.A. Grimaldeston, Z. Khalil, J.J. Finlay-Jones, Mast cells, neuropeptides, histamine, and prostaglandins in UV-induced systemic immunosuppression, *Methods* 28 (2002) 79–89.
- [38] V.E. Reeve, D. Domanski, M. Slater, Radiation sources providing increased UVA/UVB ratios induce photoprotection dependent on the UVA dose in hairless mice, *Photochem. Photobiol.* 82 (2006) 406–411.
- [39] M. Allanson, D. Domanski, V.E. Reeve, Photoimmunoprotection by UVA (320–400 nm) radiation is determined by UVA dose and is associated with cutaneous cyclic guanosine monophosphate, *J. Invest. Dermatol.* 126 (2006) 191–197.
- [40] G.J. Gendimenico, I.E. Kochevar, Degranulation of mast cells and inhibition of the response to secretory agents by phototoxic compounds and ultraviolet radiation, *Toxicol. Appl. Pharmacol.* 76 (1984) 374–382.
- [41] S. Guhl, R. Stefaniak, M. Strathmann, M. Babina, H. Plazena, B.M. Henz, T. Zuberbier, Bivalent effect of UV light on human skin mast cells-low-level mediator release at baseline but potent suppression upon mast cell triggering, *J. Invest. Dermatol.* 124 (2005) 453–456.
- [42] P. Koncz, G. Szanda, A. Rajki, A. Spät, Reactive oxygen species, Ca²⁺ signaling and mitochondrial NAD(P)H level in adrenal glomerulosa cells, *Cell Calcium* 40 (2006) 347–357.
- [43] F.X. Santos, C. Arroyo, I. Garcia, R. Blasco, J.M. Obispo, C. Hamann, L. Espejo, Role of mast cells in the pathogenesis of postburn inflammatory response: reactive oxygen species as mast cell stimulators, *Burns* 26 (2000) 145–147.
- [44] K. Wolfreys, D.B. Oliveira, Alterations in intracellular reactive oxygen species generation and redox potential modulate mast cell function, *Eur. J. Immunol.* 27 (1997) 297–306.
- [45] A.C. Brooks, C.J. Whelan, Reactive oxygen species generation by mast cells in response to substance P: a NK1-receptor-mediated event, *Inflamm. Res.* 48 (Supplement 2) (1999) S121.
- [46] E.J. Swindle, J.A. Hunt, J.W. Coleman, A comparison of reactive oxygen species generation by rat peritoneal macrophages and mast cells using the highly sensitive real-time chemiluminescent probe pholasin: inhibition of antigen-induced mast cell degranulation by macrophage-derived hydrogen peroxide, *J. Immunol.* 169 (2002) 5866–5873.
- [47] E.J. Swindle, D.D. Metcalfe, J.W. Coleman, Rodent and human mast cells produce functionally significant intracellular reactive oxygen species but not nitric oxide, *J. Biol. Chem.* 279 (2004) 48751–48759.
- [48] V.F. King, M.L. Garcia, D. Himmel, J.P. Reuben, Y.K. Lam, J.X. Pan, G.Q. Han, G.J. Kaczorowski, Interaction of tetrandrine with slowly inactivating calcium channels. Characterization of calcium channel modulation by an alkaloid of Chinese medicinal herb origin, *J. Biol. Chem.* 263 (1988) 2238–2244.
- [49] Q.Y. Liu, E. Karpinski, M.R. Rao, P.K.T. Pang, Tetrandrine: a novel calcium channel antagonist inhibits type I calcium channels in neuroblastoma cells, *Neuropharmacology* 30 (1991) 1325–1331.
- [50] C.Y. Kwan, Y.Y. Chen, M.F. Ma, E.E. Daniel, S.C.G. Hui, Tetrandrine, a calcium antagonist of Chinese herbal origin, interacts with vascular muscle α_1 -adrenoceptor, *Life Sci.* 59 (1996) 359–364.
- [51] J.W. Putney Jr., Pharmacology of capacitative calcium entry, *Mol. Interv.* 1 (2001) 84–94.
- [52] K. Imoto, H. Takemura, C.Y. Kwan, S. Sakano, M. Kaneko, H. Ohshika, Inhibitory effects of tetrandrine and hernandezine on Ca²⁺ mobilization in rat glioma C6 cells, *Res. Commun. Mol. Pathol. Pharmacol.* 95 (1997) 129–146.

- [53] S.N. Wu, H.F. Li, Y.C. Lo, Characterization of tetrandrine-induced inhibition of large-conductance calcium-activated potassium channels in a human endothelial cell line (HUV-EC-C), *J. Pharmacol. Exp. Ther.* 292 (2000) 188–195.
- [54] H.Y. Zhou, F. Wang, L. Cheng, L.Y. Fu, J. Zhou, W.X. Yao, Effects of tetrandrine on calcium and potassium currents in isolated rat hepatocytes, *World J. Gastroenterol.* 9 (2003) 134–136.
- [55] R.S. Sohal, R. Weindruch, Oxidative stress, caloric restriction, and aging, *Science* 273 (1996) 59–63.
- [56] G. Viteri, A.M. Edwards, J. De la Fuente, E. Silva, Study of the interaction between triplet riboflavin and the alpha-, betaH- and betaL-crystallins of the eye lens, *Photochem. Photobiol.* 77 (2003) 535–540.
- [57] J. Baier, T. Maisch, M. Maier, E. Engel, M. Landthaler, W. Baumler, Singlet oxygen generation by UVA light exposure of endogenous photosensitizers, *Biophys. J.* 91 (2006) 1452–1459.
- [58] J. Baier, T. Maisch, M. Maier, M. Landthaler, W. Baumler, Direct detection of singlet oxygen generated by UVA irradiation in human cells and skin, *J. Invest. Dermatol.* 127 (2007) 1498–1506.
- [59] G. Latouche, Z.G. Cerovic, F. Montagnini, I. Moya, Light-induced changes of NAD(P)H fluorescence in isolated chloroplasts: a spectral and fluorescence lifetime study, *Biochim. Biophys. Acta* 1460 (2000) 311–329.
- [60] A. Kanakubo, K. Koga, M. Isobe, K. Yoza, Tetrabromohydroquinone and riboflavin are possibly responsible for green luminescence in the luminous acorn worm, *Ptychodera flava*, *Luminescence* 20 (2005) 397–400.
- [61] S. Zhuang, I.E. Kochevar, Ultraviolet A radiation induces rapid apoptosis of human leukemia cells by Fas ligand-independent activation of the Fas death pathways, *Photochem. Photobiol.* 78 (2003) 61–67.
- [62] S. Gross, A. Knebel, T. Tenev, A. Neining, M. Gaestel, P. Herrlich, F.D. Bohmer, Inactivation of protein-tyrosine phosphatases as mechanism of UV-induced signal transduction, *J. Biol. Chem.* 274 (1999) 26378–26386.
- [63] C. Blanchetot, L.G. Tertoolen, J. den Hertog, Regulation of receptor protein-tyrosine phosphatase alpha by oxidative stress, *EMBO J.* 21 (2002) 493–503.
- [64] N. Wang, Y. Liu, M.X. Xie, Z.J. Cui, Changes in plasma membrane protein structure after photodynamic action in freshly isolated rat pancreatic acini. An FTIR study, *J. Photochem. Photobiol.* 71 (2003) 27–34.
- [65] E.J. Swindle, J.W. Coleman, F.R. DeLeo, D.D. Metcalfe, FcepsilonRI- and Fcgamma receptor-mediated production of reactive oxygen species by mast cells is lipoxygenase- and cyclooxygenase-dependent and NADPH oxidase-independent, *J. Immunol.* 179 (2007) 7059–7071.